Intimate Relationship Between Sterile Neutrino Dark Matter and ΔN_{eff}

Kevin J. Kelly,[1, *] Manibrata Sen,[2, 3, †] and Yue Zhang[4, ‡]

[1] *Theory Department, Fermi National Accelerator Laboratory, Batavia, IL 60510, USA*
[2] *Department of Physics, University of California Berkeley, Berkeley, CA 94720, USA*
[3] *Department of Physics & Astronomy, Northwestern University, Evanston, IL 60208, USA*
[4] *Department of Physics, Carleton University, Ottawa, ON K1S 5B6, Canada*
(Dated: November 6, 2020)

The self-interacting neutrino hypothesis is well motivated for addressing the tension between the origin of sterile neutrino dark matter and indirect detection constraints. It can also result in a number of testable signals from the laboratories to the cosmos. We explore a model of neutrino self-interaction mediated by a Majoron-like scalar with sub-MeV mass, and show that explaining the relic density of sterile neutrino dark matter implies a lower bound on the amount of extra radiation in early universe, in particular $\Delta N_{\text{eff}} > 0.12$ at the CMB epoch. This lower bound will be further strengthened with an improved X-ray search at the Athena observatory. Such an intimate relationship will be unambiguously tested by the upcoming CMB-S4 project.

Introduction – The nature of dark matter (DM) is one of the most fascinating puzzles of our Universe. A sterile neutrino with a keV-scale mass and a small mixing with the active neutrinos is a simple and well-motivated DM candidate – it is also a highly testable one. In the minimal setup, the active-sterile neutrino mixing that can account for the observed DM relic density [1] is already in strong tension with indirect detection results searching for DM decaying into monochromatic X-ray (see [2] for a review). Among the various proposals to alleviate this tension is the active neutrino self-interactions mediated by a new force. This provides an elegant solution which keeps neutrinos in thermal equilibrium with themselves longer in the early Universe and facilitates more efficient sterile neutrino DM (SνDM) production [3, 4]. Such a new interaction leads to a number of signatures for it to be probed in laboratories, e.g., at beam neutrino facilities [5]. If the mediator is heavier than $\sim$MeV, it decouples from neutrinos before big-bang nucleosynthesis (BBN) leaving the remaining evolution of the Universe intact.

By the end of this decade, we will enter a new precision era of cosmology. The Cosmic Microwave Background - Stage 4 (CMB-S4) project [6] is expected to measure cosmological parameters to an unprecedented high-precision level. In particular, it could restrict the amount of extra radiation (in units of extra neutrinos, ΔN_{eff}) during the CMB epoch to a few-percent uncertainty, while it is still allowed (perhaps even favored) to be order one by the current data [7, 8]. This could shed light on existing tensions resulting from various ways of measuring the Hubble parameter [9–12], as well as fundamental theories that can accommodate deviations from the standard cosmology.

In this letter, we point out an intriguing relationship between the two important ingredients of our Universe – the origin of SνDM and ΔN_{eff}. Such an observation is made in the context of self-interacting neutrino models with an ultra-light scalar mediator below the MeV scale.

The mediator possesses a feeble coupling to active neutrinos such that it enters the thermal bath after BBN but decays away before CMB. We identify the parameter space where SνDM is dominantly produced from active neutrino self scattering through the exchange of on-shell mediator. Meanwhile, the post-BBN thermalization of the mediator inevitably modifies the standard cosmology predictions by making new contributions to ΔN_{eff} for both CMB and BBN. As a result, the viable parameter space for SνDM relic density is highly correlated with the values of ΔN_{eff}. We further point out a new implication of the upcoming indirect DM search by the Athena experiment for the next-generation precision measurements in cosmology.

Models – SνDM is a linear combination of a gauge singlet fermion and the active neutrino states from the Standard Model [1],

$$\nu_4 = \nu_s \cos\theta + \nu_a \sin\theta ,\tag{1}$$

where ν_4 denotes a mass eigenstate and θ is the active-sterile mixing angle in vacuum. The sterile neutrino is a decaying DM candidate whose longevity is attributed to its small mass ($m_4 \gtrsim$ keV) and mixing ($\theta \ll 1$). In addition, we introduce a new force among active neutrinos mediated by a spin-zero boson ϕ,

$$\mathcal{L}_{\text{int.}} = \frac{\lambda_{\alpha\beta}}{2}\nu_\alpha\nu_\beta\phi + \text{h.c.} , \quad (\alpha, \beta = e, \mu, \tau) ,\tag{2}$$

which can be obtained from dimension-six gauge invariant operators at energy scales well below the weak scale. The scalar field ϕ could be either real or complex. In the former case, ϕ could be identified as the Majoron [13, 14], where $\lambda = iM_\nu/f$ and f is the spontaneous lepton number breaking scale, whereas in the latter case, ϕ also contains the radial mode and restores the $B - L$ symmetry at high scales [15]. The two choices feature qualitatively similar but quantitatively different predictions in cosmology due to the extra degrees of freedom from a complex scalar. Furthermore, a real scalar ϕ could thermalize with

both neutrinos and antineutrinos, whereas a complex ϕ (ϕ^*) only couple to neutrinos (antineutrinos).

The impact of active neutrino self-interactions on the DM relic density was first observed in [3]. The new force enables more frequent active neutrino scattering than normal weak interactions. As a result, SνDM can be produced with a smaller mixing angle than required by Dodelson and Widrow [1]. In particular, Ref. [3] focuses on m_ϕ between MeV–GeV, where the new interaction is always sufficiently strong to fully thermalize ϕ before BBN. In this region, the strongest probes come from the laboratories, including accurate meson decay measurements [15–17] and accelerator neutrino experiments [5]. For m_ϕ close to MeV, the parameter space for relic density runs into conflict with BBN due to ϕ's contribution to ΔN_{eff}.

The present work focuses on SνDM production with a ϕ mass well below MeV. Such a possibility can be consistent with BBN if ϕ does not thermalize during the BBN era and has no primordial population from other high scale physics [18–26]. The non-thermalization of ϕ is due to a feeble ϕ-ν coupling and/or a phase space suppression for the process $\nu\nu \to \phi$ to occur at temperatures much higher than m_ϕ. Later on, ϕ can still have a strong impact on SνDM production, once it establishes a thermal equilibrium with active neutrinos. The condition for not thermalizing ϕ before BBN sets an upper bound on λ that scales as $1/m_\phi$, whereas correct DM relic density requires λ to scale as $\sqrt{m_\phi}$ in the small coupling regime. As a result, a viable parameter space opens up for m_ϕ between keV–MeV.

Cosmology – The production of SνDM is governed by the equation

$$\frac{df_4(E,z)}{dz} = \frac{\Gamma(E,z)\sin^2 2\theta}{4Hz} f_a(E,z)\Theta(E-m_4) , \quad (3)$$

where f_4 and f_a are phase space distribution functions of sterile and active neutrinos, respectively. The argument $z \equiv m_\phi/T_\nu^{\mathrm{sc}}$ is introduced to label time in the early Universe, where T_ν^{sc} is defined as the neutrino temperature in the standard cosmology without ϕ; thus z literally expands linearly with the radius of the Universe. In contrast, the actual neutrino temperature T_ν is affected by the interaction introduced in Eq. (2). After weak interaction decoupling, it deviates from T_ν^{sc} as the population of ϕ builds up. On the right-hand side, Γ is the thermal-averaged scattering rate for an active neutrino with energy E, and H is the Hubble parameter. We are mainly interested in a light ϕ that is weakly coupled to neutrinos. To a very good approximation, the effective active-sterile mixing angle is equal to the vacuum one throughout the dominant production window (below MeV).

The distribution function f_a, after active neutrinos reach thermal equilibrium with ϕ, is characterized by

their temperature T_ν and a chemical potential μ_ν,

$$f_a(E,z) = \frac{1}{1 + \exp\left[(E - \mu_\nu(z))/T_\nu(z)\right]} . \quad (4)$$

To derive their z dependence, we introduce three time scales in the early Universe,

- z_A: the onset of BBN where neutrinos have just decoupled from weak interaction. Following our assumption, ϕ has not reached equilibrium with neutrinos yet;

- z_B: the ν-ϕ system has just established thermal equilibrium. In most of the parameter space we explore, ϕ remains ultra-relativistic at this moment;

- z_C: all ϕ particles have decayed away ($T \ll m_\phi$), mostly into neutrinos, with a small fraction decaying into SνDM.

Prior to z_A, neutrinos and the photon share the same temperature $T_\nu = T_\nu^{\mathrm{sc}} = T_\gamma$. The ν-ϕ interaction freezes in a sub-thermal population of ϕ via the Boltzmann equation

$$\frac{dY_\phi}{dz} = -\frac{\gamma_{\phi\leftrightarrow\nu\nu}}{sHz}\left(\frac{Y_\phi}{Y_\phi^{\mathrm{EQ}}} - 1\right) , \quad (5)$$

where $Y_\phi = n_\phi/s$ is the yield, n_ϕ is the number density of ϕ, and s is the entropy density of the Universe. The thermal averaged rate is $\gamma_{\phi\to\nu\nu} \simeq m_\phi^3 \Gamma_\phi/(2\pi^2 z^2)$ in the small m_ϕ limit, where $\Gamma_\phi = 3\lambda^2 m_\phi/(32\pi)$. [1] Here we assume ϕ couples universally to three neutrino flavors, $\lambda_{ee,\mu\mu,\tau\tau} = \lambda$. Generalization to other flavor structures will be addressed later on. Assuming no ϕ population at early times ($z \ll z_A$), we integrate Eq. (5) up to z_A to derive the population of ϕ which contributes to $\Delta N_{\mathrm{eff}}^{\mathrm{BBN}}$.

Between z_A and z_B, the ν-ϕ interaction takes them to chemical equilibrium. At z_B, the neutrino temperature T_ν deviates from T_ν^{sc}; a chemical potential is also generated with relation, $\mu_\phi = 2\mu_\nu = 2\mu_{\bar\nu}$ for real scalar ϕ, or $\mu_\phi = 2\mu_\nu$ and $\mu_{\phi^*} = 2\mu_{\bar\nu}$ for complex ϕ. Without CP violation, $\mu_\phi = \mu_\phi^*$. At time z_B, the values of T_ν and μ_ν are dictated by energy and lepton number conservation laws [29–31]. In the supplemental material A, we provide the details of this matching. Entropy is not preserved here because the ϕ thermalization process is irreversible.

The most important epoch for SνDM production is between z_B and z_C, by the $\nu\nu \to \nu\nu_4$ process with an on-shell ϕ exchange in the s-channel. This process is terminated after ϕ becomes non-relativistic and freezes out

---

[1] The $\nu\bar\nu \to \phi\phi^{(*)}$ process is only important for the coupling λ much larger than those of interest to this work [27, 28].
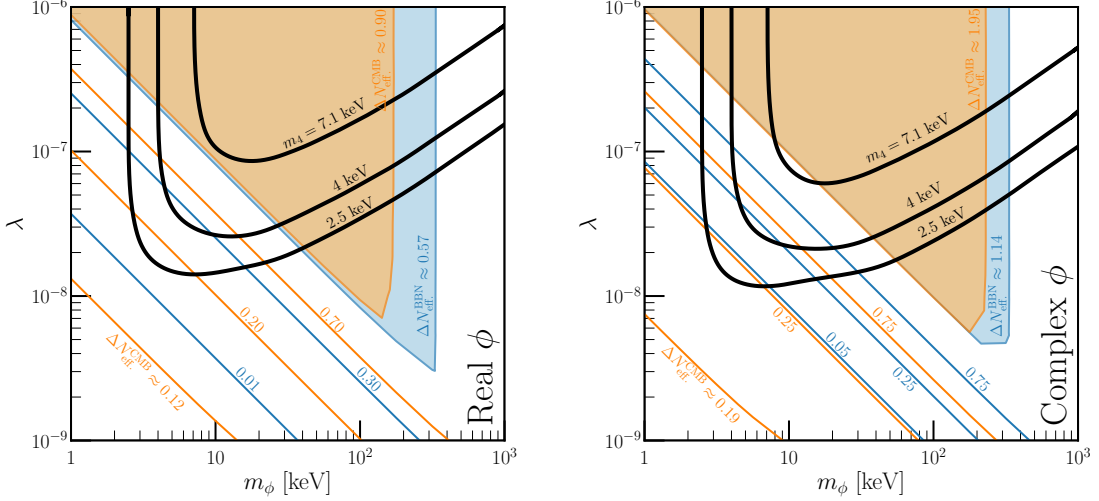
FIG. 1. Sterile neutrino DM relic density (black contours) and ΔN_{eff} (orange and blue contours for CMB and BBN, respectively), as a function of λ and m_ϕ for real (left) and complex (right) scalar ϕ. We present three choices of the SνDM mass with the largest experimentally allowed mixing angles (see main text).

of the Universe. The entropy and lepton number conservation laws allow us to derive the functions $T_\nu(z)$ and $\mu_\nu(z)$. The total energy of the Universe thereby increases because part of the ϕ particles decay while turning non-relativistic. The neutrino self interaction rate Γ also depends on $T_\nu(z)$ and $\mu_\nu(z)$,

$$
\Gamma(E, z) = \frac{3\lambda^2 m_\phi^2 T_\nu e^{\mu_\nu/T_\nu}}{4\pi E^2}
$$
$$
\times \left[e^{-\omega} + \sqrt{\frac{\pi}{4\omega}} \text{erfc}\left(\sqrt{\omega}\right) \right] \sqrt{1 - \frac{m_4^2}{m_\phi^2}} , \quad (6)
$$

where $\omega = m_\phi^2/(4ET_\nu)$. With the above results, we integrate Eq. (3) up to z_C to obtain the corresponding relic abundance of SνDM ν_4 using

$$
\Omega_4 = \frac{m_4 s_0}{2\pi^2 s(z_C)\rho_0} \int_{m_4}^{\infty} E dE \sqrt{E^2 - m_4^2} f_4(E, z_C) , \quad (7)
$$

where $s_0 = 2891.2 \,\text{cm}^{-3}$ and $\rho_0 = 1.05 \times 10^{-5} \, h^{-2} \,\text{GeV/cm}^3$ are entropy and critical energy densities of the Universe today [32]. The total entropy density at time z_C (in practice z_C is set to 30) is

$$
s(z_C) = \frac{2\pi^2}{45} \left[2T_\gamma^3 + 2s_\nu\left(T_\nu(z_C), \mu_\nu(z_C)\right) \right] , \quad (8)
$$

where $T_\gamma \simeq 1.39 T_\nu^{\text{SC}} = 1.39 m_\phi/z_C$, and

$$
s_\nu(T_\nu, \mu_\nu) = -\frac{3}{\pi^2} \left[4\text{Li}_4(-e^{\mu_\nu/T_\nu}) - \frac{\mu_\nu}{T_\nu} \text{Li}_3(-e^{\mu_\nu/T_\nu}) \right] . \quad (9)
$$

The early-Universe ν-ϕ sector described above also allows one to calculate the other important quantity in cosmology, ΔN_{eff}, which encodes additional contributions to

the expansion rate of the Universe. ΔN_{eff} is measured at both BBN and CMB epochs. A positive $\Delta N_{\text{eff}}^{\text{BBN}}$ is generated by the non-thermal production of ϕ at temperatures above the MeV scale,

$$
\Delta N_{\text{eff}}^{\text{BBN}} \simeq 3.046 \left(\frac{\rho_\phi(z_A)}{\rho_\nu(z_A)} \right) , \quad (10)
$$

where $\rho_\nu(z_A) = 9\zeta(3)T_\nu(z_A)^4/(4\pi^2)$ and $\rho_\phi(z_A)$ can be calculated by solving Eq. (5). The thermal reaction rate $\gamma_{\phi \leftrightarrow \nu\nu}$ is proportional to $(\lambda m_\phi)^2$, implying weaker BBN constraints for light ϕ.

By the time of CMB, ϕ particles have become heavy and already decayed away. The contribution to $\Delta N_{\text{eff}}^{\text{CMB}}$ is due to the non-standard distribution function of active neutrinos, and can be calculated using

$$
\Delta N_{\text{eff}}^{\text{CMB}} = 3.046 \left(\frac{\rho_\nu}{\rho_\nu^{\text{SC}}} - 1 \right) . \quad (11)
$$

where

$$
\frac{\rho_\nu}{\rho_\nu^{\text{SC}}} = -\frac{720}{7\pi^4} \left(\frac{T_\nu(z_C)}{T_\nu^{\text{SC}}(z_C)} \right)^4 \text{Li}_4(-e^{\mu_\nu(z_C)/T_\nu(z_C)}) . \quad (12)
$$

The production of SνDM via active-sterile mixing also leads to a slight reduction in the active neutrino population. However, given the much lower number density of SνDM compared to that of neutrinos, this effect only modifies $\Delta N_{\text{eff}}^{\text{CMB}}$ by less than one percent.

In short, neutrino self interactions in the early universe via an ultra-light mediator ϕ imply a tight correlation between the origin of SνDM and the amount of extra radiation. The post-BBN thermalization of ϕ provides a novel mechanism that accounts for the correct relic density of SνDM. Meanwhile, the ϕ thermalization distorts

the phase space distribution of active neutrinos, leading to a net $\Delta N_{\text{eff}} > 0$ for both CMB and BBN epochs. It is then of great phenomenological interest to quantify such an interplay, especially the prediction for $\Delta N_{\text{eff}}^{\text{CMB}}$, which will serve as a well-motivated target for the upcoming CMB-S4 test.

Results and Discussions – To present the numerical results, we first select three SνDM masses, $m_4 = \{2.5, 4, 7.1\}\,\text{keV}$, together with the correspondingly largest active-sterile mixing parameter, $\sin^2 2\theta \simeq \{5 \times 10^{-9}, 10^{-9}, 7 \times 10^{-11}\}$, that is consistent with current X-ray search limits [2, 33–35]. In Fig. 1, we scan over the λ versus m_ϕ parameter space, focusing on m_ϕ between keV and MeV, and derive the black solid curves that can account for the observed DM relic abundance, $\Omega_{\nu_4} h^2 = 0.1186$. For $m_\phi \gg m_4$, all the curves feature a constant slope, $\lambda \sim m_\phi^{1/2}$, which matches to result in the $m_\phi \gtrsim 1\,\text{MeV}$ region [3]. For m_ϕ close to m_4, all the curves bend up, where larger coupling λ is required to compensate for the phase space suppression of the $\phi \to \nu\nu_4$ decay. In the same figure, we also present contours of constant $\Delta N_{\text{eff}}^{\text{BBN}}$ and $\Delta N_{\text{eff}}^{\text{CMB}}$ values generated by the ϕ-ν interaction. Their intersections with the DM relic density contour dictate the correlation between Ω_4 and ΔN_{eff}. For real (complex) scalar ϕ, we find the following predictions $0 < \Delta N_{\text{eff}}^{\text{BBN}} < 0.57$ and $0.12 < \Delta N_{\text{eff}}^{\text{CMB}} < 0.9$ ($0 < \Delta N_{\text{eff}}^{\text{BBN}} < 1.14$ and $0.19 < \Delta N_{\text{eff}}^{\text{CMB}} < 1.95$). The maximal values correspond to strong coupling limit with ϕ fully thermalized by the time of BBN, whereas the minimal values correspond to sufficiently small λ and/or m_ϕ and negligible pre-BBN population of ϕ. In the lower-left half of each λ-m_ϕ plane, both $\Delta N_{\text{eff}}^{\text{BBN}}$ and $\Delta N_{\text{eff}}^{\text{CMB}}$ follow the same parametrical dependence as the ϕ production rate $\gamma_{\phi \leftrightarrow \nu\nu}$ in Eq. (5) and depend only on the product (λm_ϕ). The state-of-art upper bound on $\Delta N_{\text{eff}}^{\text{BBN}} \lesssim 0.5$ [36] marginally excludes the fully-thermalized real ϕ case prior to BBN and sets a stronger constraint for complex ϕ.

Contrasting the SνDM relic density and ΔN_{eff} curves in Fig. 1, we find that for each DM mass one can derive the corresponding lowest values of $\Delta N_{\text{eff}}^{\text{BBN}}$ and $\Delta N_{\text{eff}}^{\text{CMB}}$. Reducing the active-sterile mixing angle θ would require larger coupling λ to maintain the desired relic density and result in even higher values of $\Delta N_{\text{eff}}^{\text{BBN}}$ and $\Delta N_{\text{eff}}^{\text{CMB}}$ until they saturate to the corresponding maximum. Remarkably, correct SνDM relic density predicts minimal ΔN_{eff}. This is clearly a nice target for precision BBN and CMB measurements. Moreover, because the angle θ is more strongly constrained for higher SνDM mass, an upper bound on ΔN_{eff} could in turn set an upper bound on DM mass. This forms a novel interplay with DM indirect detection experiments. Inspired by this observation, we present Fig. 2. For each DM mass, we combine the current X-ray constraint and the relic density requirement to derive minimal values of $\Delta N_{\text{eff}}^{\text{BBN}}$ and $\Delta N_{\text{eff}}^{\text{CMB}}$, as shown

in the left panel. We refer to supplemental material B for more details. Interestingly, we find a lower bound, $\Delta N_{\text{eff}}^{\text{CMB}} > 0.12$, given the existing constraints on sterile neutrino dark matter, which is a very nice target for the CMB-S4 experiment. For large enough $m_4 \gtrsim 6\,\text{keV}$, $\Delta N_{\text{eff}}^{\text{BBN}}$ and $\Delta N_{\text{eff}}^{\text{CMB}}$ have already saturated to the their maximal values. The right panel of Fig. 2 shows the impact of future measurement of the active-sterile mixing $\sin^2 2\theta$ by the Athena X-ray observatory [37] on ΔN_{eff}. With stronger sensitivity to $\sin^2 2\theta$, DM relic density sets higher minimal values of $\Delta N_{\text{eff}}^{\text{BBN}}$ and $\Delta N_{\text{eff}}^{\text{CMB}}$, in particular, $\Delta N_{\text{eff}}^{\text{CMB}} > 0.3$. These predictions will be robustly tested by the upcoming CMB-S4 experiment, with the uncertainty in $\Delta N_{\text{eff}}^{\text{CMB}}$ measurement narrowed down to a few percent level. The two classes of probes are highly complementary and will further narrow down the parameter space of SνDM.

The range of SνDM mass shown in Fig. 2 is $2\,\text{keV} < m_4 < 10\,\text{keV}$. Lower values of m_4 are inconsistent with the phase space density constraint from dwarf galaxies [2, 38, 39]. A stronger lower bound on m_4 may be set using Lyman-α forest [40] as well as Milky Way satellite dwarf galaxy counts [41]. However, in this model, the DM free-streaming length can be substantially shorter than regular warm DM. In a numerical calculation, we notice that SνDM is always dominantly produced around $z \sim 3 - 4$ where ϕ already starts to turn non-relativistic (see Fig. 4 in supplemental material A). The initial DM velocity is thus suppressed if m_ϕ and m_4 are close. Interestingly, such a near-degeneracy exactly occurs where ΔN_{eff} is minimized (see Fig. 1). As a result, small scale constraints are relaxed.

So far we have assumed that ϕ couples equally to all the active neutrinos. Our conclusions remain qualitatively the same if this assumption is relaxed to flavor non-universal and/or off-diagonal couplings. By the time of ϕ thermalization, there is sufficient time in early Universe for neutrino flavor conversions (via e.g. oscillation and decoherence) to occur, which necessarily equilibrates ϕ with all active neutrinos, unless the ϕ coupling is judiciously chosen to couple to a particular mass eigenstate.

Before closing, we comment on other relevant constraints. A light mediator ϕ exchange leads to new SνDM decay channel $\nu_4 \to 3\nu$ which could substantially shorten its lifetime [3]. In the parameter space relevant to this study (Fig. 1), DM is still much longer-lived than the age of Universe. The neutrinos from SνDM decay are a potential indirect detection target. A sub-MeV ϕ that couples to the electron neutrino of the form Eq. (2) can affect the two-neutrino double-beta ($2\nu2\beta$) decay rate. The current $2\nu2\beta$ limit, $\lambda \lesssim 10^{-4}$ [42–44], lies well above Fig. 1. The ϕ-ν coupling is also constrained by the cooling argument of core-collapsing supernovae [45]. The constraints found in Refs. [44, 46, 47] is comparable to (for $\lambda_{\mu\mu}, \lambda_{\tau\tau}$ couplings slightly weaker than) that of BBN for $m_\phi \ll \text{MeV}$.
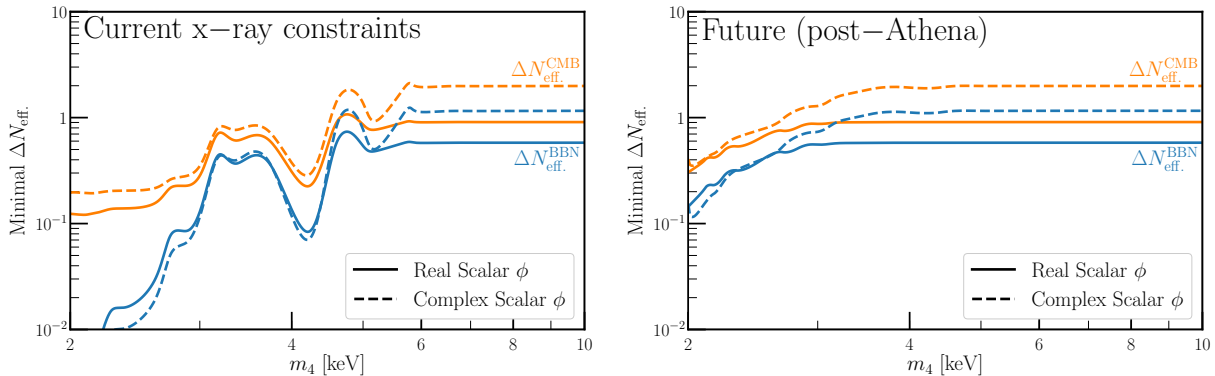
FIG. 2. Minimal value of ΔN_{eff} at the time of CMB (orange) and BBN (blue) as a function of SνDM mass m_4. All contours correspond to the largest allowed active-sterile mixing parameter $\sin^2(2\theta)$ by the current (left) and upcoming (right) searches of X-ray line from $\nu_4 \to \nu\gamma$ decay.

In summary, we explore the impact of active neutrino self interaction, mediated by an ultralight scalar ϕ, on the relic density of SνDM and the amount of extra radiation (ΔN_{eff}) in the early Universe. Strong neutrino self interactions in the early Universe can facilitate efficient production of DM and generate a net ΔN_{eff} at the same time. Our study reveals an intimate relationship between these two important quantities and provide a well-motivated target for the future cosmological and astrophysical experiments, including CMS-S4 and Athena. Recent analysis of the present cosmological data showed a slight preference of $\Delta N_{\text{eff}}^{\text{CMB}} > 0$ and a sizable neutrino self interacting cross section [48–50]. Our model is able to accommodate the desired values of ΔN_{eff} but not as large of a cross section. Such a hint for new physics will soon get tested by CMB-S4. On the theory side, if ϕ is the Majoron, a discovery of SνDM and the corresponding neutrino self interaction strength will determine the spontaneous lepton number breaking scale. One could also consider a similar framework with neutrino self interaction mediated by a vector boson [4, 51], such as gauged $U(1)_{\mu-\tau}$. However, the parameter space for SνDM production is already more tightly constrained for a sub-MeV vector mediator [52].

* kkelly12@fnal.gov, ORCID: 0000-0002-4892-2093
† manibrata@berkeley.edu, ORCID: 0000-0001-7948-4332
‡ yzhang@physics.carleton.ca, ORCID: 0000-0002-1984-7450

[1] Scott Dodelson and Lawrence M. Widrow, "Sterile-neutrinos as dark matter," Phys. Rev. Lett. **72**, 17–20 (1994), arXiv:hep-ph/9303287 [hep-ph].

[2] Kevork N. Abazajian, "Sterile neutrinos in cosmology," Phys. Rept. **711-712**, 1–28 (2017), arXiv:1705.01837 [hep-ph].

[3] André De Gouvêa, Manibrata Sen, Walter Tangarife, and Yue Zhang, "The Dodelson-Widrow Mechanism In the Presence of Self-Interacting Neutrinos," Phys. Rev. Lett. **124**, 081802 (2020), arXiv:1910.04901 [hep-ph].

[4] Kevin J. Kelly, Manibrata Sen, Walter Tangarife, and Yue Zhang, "Origin of sterile neutrino dark matter via secret neutrino interactions with vector bosons," Phys. Rev. D **101**, 115031 (2020), arXiv:2005.03681 [hep-ph].

[5] Kevin J. Kelly and Yue Zhang, "Mononeutrino at DUNE: New Signals from Neutrinophilic Thermal Dark Matter," Phys. Rev. **D99**, 055034 (2019), arXiv:1901.01259 [hep-ph].

[6] Kevork N. Abazajian et al. (CMB-S4), "CMB-S4 Science Book, First Edition," (2016), arXiv:1610.02743 [astro-ph.CO].

[7] P.A.R. Ade et al. (Planck), "Planck 2015 results. XIII. Cosmological parameters," Astron. Astrophys. **594**, A13 (2016), arXiv:1502.01589 [astro-ph.CO].

[8] Jose Luis Bernal, Licia Verde, and Adam G. Riess, "The trouble with H_0," JCAP **10**, 019 (2016), arXiv:1607.05617 [astro-ph.CO].

[9] Wendy L. Freedman, "Cosmology at a Crossroads," Nature Astron. **1**, 0121 (2017), arXiv:1706.02739 [astro-ph.CO].

[10] Kenneth C. Wong et al., "H0LiCOW XIII. A 2.4% measurement of H_0 from lensed quasars: 5.3σ tension between early and late-Universe probes," (2019), 10.1093/mnras/stz3094, arXiv:1907.04869 [astro-ph.CO].

[11] Adam G. Riess, Stefano Casertano, Wenlong Yuan, Lucas M. Macri, and Dan Scolnic, "Large Magellanic Cloud Cepheid Standards Provide a 1% Foundation for the Determination of the Hubble Constant and Stronger Evidence for Physics beyond ΛCDM," Astrophys. J. **876**, 85

(2019), arXiv:1903.07603 [astro-ph.CO].

[12] N. Aghanim *et al.* (Planck), "Planck 2018 results. VI. Cosmological parameters," Astron. Astrophys. **641**, A6 (2020), arXiv:1807.06209 [astro-ph.CO].

[13] Y. Chikashige, Rabindra N. Mohapatra, and R.D. Peccei, "Spontaneously Broken Lepton Number and Cosmological Constraints on the Neutrino Mass Spectrum," Phys. Rev. Lett. **45**, 1926 (1980).

[14] G.B. Gelmini and M. Roncadelli, "Left-Handed Neutrino Mass Scale and Spontaneously Broken Lepton Number," Phys. Lett. B **99**, 411–415 (1981).

[15] Jeffrey M. Berryman, André De Gouvêa, Kevin J. Kelly, and Yue Zhang, "Lepton-Number-Charged Scalars and Neutrino Beamstrahlung," Phys. Rev. **D97**, 075030 (2018), arXiv:1802.00009 [hep-ph].

[16] Nikita Blinov, Kevin James Kelly, Gordan Z Krnjaic, and Samuel D McDermott, "Constraining the Self-Interacting Neutrino Interpretation of the Hubble Tension," Phys. Rev. Lett. **123**, 191102 (2019), arXiv:1905.02727 [astro-ph.CO].

[17] Vedran Brdar, Manfred Lindner, Stefan Vogl, and Xun-Jie Xu, "Revisiting Neutrino Self-Interaction Constraints from Z and τ decays," (2020), arXiv:2003.05339 [hep-ph].

[18] Xiang-Dong Shi and George M. Fuller, "A New dark matter candidate: Nonthermal sterile neutrinos," Phys. Rev. Lett. **82**, 2832–2835 (1999), arXiv:astro-ph/9810076 [astro-ph].

[19] Mikhail Shaposhnikov and Igor Tkachev, "The nuMSM, inflation, and dark matter," Phys. Lett. B **639**, 414–417 (2006), arXiv:hep-ph/0604236.

[20] Takehiko Asaka, Mikhail Shaposhnikov, and Alexander Kusenko, "Opening a new window for warm dark matter," Phys. Lett. B **638**, 401–406 (2006), arXiv:hep-ph/0602150.

[21] Samuel B. Roland, Bibhushan Shakya, and James D. Wells, "Neutrino Masses and Sterile Neutrino Dark Matter from the PeV Scale," Phys. Rev. D **92**, 113009 (2015), arXiv:1412.4791 [hep-ph].

[22] Rasmus S. L. Hansen and Stefan Vogl, "Thermalizing sterile neutrino dark matter," Phys. Rev. Lett. **119**, 251305 (2017), arXiv:1706.02707 [hep-ph].

[23] Lucas Johns and George M. Fuller, "Self-interacting sterile neutrino dark matter: the heavy-mediator case," Phys. Rev. D **100**, 023533 (2019), arXiv:1903.08296 [hep-ph].

[24] F. Bezrukov, H. Hettmansperger, and M. Lindner, "keV sterile neutrino Dark Matter in gauge extensions of the Standard Model," Phys. Rev. D **81**, 085032 (2010), arXiv:0912.4415 [hep-ph].

[25] Miha Nemevsek, Goran Senjanovic, and Yue Zhang, "Warm Dark Matter in Low Scale Left-Right Theory," JCAP **07**, 006 (2012), arXiv:1205.0844 [hep-ph].

[26] Jeff A. Dror, David Dunsky, Lawrence J. Hall, and Keisuke Harigaya, "Sterile Neutrino Dark Matter in Left-Right Theories," (2020), arXiv:2004.09511 [hep-ph].

[27] Guo-yuan Huang, Tommy Ohlsson, and Shun Zhou, "Observational Constraints on Secret Neutrino Interactions from Big Bang Nucleosynthesis," Phys. Rev. D **97**, 075009 (2018), arXiv:1712.04792 [hep-ph].

[28] Gabriela Barenboim and Ulrich Nierste, "Modified majoron model for cosmological anomalies," (2020), arXiv:2005.13280 [hep-ph].

[29] Z. Chacko, Lawrence J. Hall, Takemichi Okui, and Steven J. Oliver, "CMB signals of neutrino mass generation," Phys. Rev. D **70**, 085008 (2004), arXiv:hep-ph/0312267.

[30] Miguel Escudero Abenza, "Precision early universe thermodynamics made simple: $N_{\rm eff}$ and neutrino decoupling in the Standard Model and beyond," JCAP **05**, 048 (2020), arXiv:2001.04466 [hep-ph].

[31] Asher Berlin and Nikita Blinov, "Thermal Dark Matter Below an MeV," Phys. Rev. Lett. **120**, 021801 (2018), arXiv:1706.07046 [hep-ph].

[32] P.A. Zyla *et al.* (Particle Data Group), "Review of Particle Physics," PTEP **2020**, 083C01 (2020).

[33] Shunsaku Horiuchi, Philip J. Humphrey, Jose Onorbe, Kevork N. Abazajian, Manoj Kaplinghat, and Shea Garrison-Kimmel, "Sterile neutrino dark matter bounds from galaxies of the Local Group," Phys. Rev. D **89**, 025017 (2014), arXiv:1311.0282 [astro-ph.CO].

[34] D. Malyshev, A. Neronov, and D. Eckert, "Constraints on 3.55 keV line emission from stacked observations of dwarf spheroidal galaxies," Phys. Rev. D **90**, 103506 (2014), arXiv:1408.3531 [astro-ph.HE].

[35] Christopher Dessert, Nicholas L. Rodd, and Benjamin R. Safdi, "The dark matter interpretation of the 3.5-keV line is inconsistent with blank-sky observations," Science **367**, 1465 (2020), arXiv:1812.06976 [astro-ph.CO].

[36] Cyril Pitrou, Alain Coc, Jean-Philippe Uzan, and Elisabeth Vangioni, "Precision big bang nucleosynthesis with improved Helium-4 predictions," Phys. Rept. **754**, 1–66 (2018), arXiv:1801.08023 [astro-ph.CO].

[37] A. Neronov and D. Malyshev, "Toward a full test of the νMSM sterile neutrino dark matter model with Athena," Phys. Rev. D **93**, 063518 (2016), arXiv:1509.02758 [astro-ph.HE].

[38] S. Tremaine and J.E. Gunn, "Dynamical Role of Light Neutral Leptons in Cosmology," Phys. Rev. Lett. **42**, 407–410 (1979).

[39] Alexey Boyarsky, Oleg Ruchayskiy, and Dmytro Iakubovskyi, "A Lower bound on the mass of Dark Matter particles," JCAP **03**, 005 (2009), arXiv:0808.3902 [hep-ph].

[40] Christophe Yèche, Nathalie Palanque-Delabrouille, Julien Baur, and Hélion du Mas des Bourboux, "Constraints on neutrino masses from Lyman-alpha forest power spectrum with BOSS and XQ-100," JCAP **06**, 047 (2017), arXiv:1702.03314 [astro-ph.CO].

[41] E.O. Nadler *et al.* (DES), "Milky Way Satellite Census. III. Constraints on Dark Matter Properties from Observations of Milky Way Satellite Galaxies," (2020), arXiv:2008.00022 [astro-ph.CO].

[42] M. Agostini *et al.*, "Results on $\beta\beta$ decay with emission of two neutrinos or Majorons in ^{76} Ge from GERDA Phase I," Eur. Phys. J. C **75**, 416 (2015), arXiv:1501.02345 [nucl-ex].

[43] Kfir Blum, Yosef Nir, and Michal Shavit, "Neutrinoless double-beta decay with massive scalar emission," Phys. Lett. B **785**, 354–361 (2018), arXiv:1802.08019 [hep-ph].

[44] Tim Brune and Heinrich Päs, "Massive Majorons and constraints on the Majoron-neutrino coupling," Phys. Rev. D **99**, 096005 (2019), arXiv:1808.08158 [hep-ph].

[45] G.G. Raffelt, *Stars as laboratories for fundamental physics: The astrophysics of neutrinos, axions, and other weakly interacting particles* (1996).

[46] Lucien Heurtier and Yongchao Zhang, "Supernova Constraints on Massive (Pseudo)Scalar Coupling to Neutri-

nos," JCAP **02**, 042 (2017), arXiv:1609.05882 [hep-ph].

[47] Miguel Escudero, Jacobo Lopez-Pavon, Nuria Rius, and Stefan Sandner, "Relaxing Cosmological Neutrino Mass Bounds with Unstable Neutrinos," (2020), arXiv:2007.04994 [hep-ph].

[48] Francesco Forastieri, Massimiliano Lattanzi, and Paolo Natoli, "Constraints on secret neutrino interactions after Planck," JCAP **07**, 014 (2015), arXiv:1504.04999 [astro-ph.CO].

[49] Francesco Forastieri, Massimiliano Lattanzi, and Paolo Natoli, "Cosmological constraints on neutrino self-interactions with a light mediator," Phys. Rev. D **100**, 103526 (2019), arXiv:1904.07810 [astro-ph.CO].

[50] Christina D. Kreisch, Francis-Yan Cyr-Racine, and Olivier Doré, "The Neutrino Puzzle: Anomalies, Interactions, and Cosmological Tensions," (2019), arXiv:1902.00534 [astro-ph.CO].

[51] Brian Shuve and Itay Yavin, "Dark matter progenitor: Light vector boson decay into sterile neutrinos," Phys. Rev. D **89**, 113004 (2014), arXiv:1403.2727 [hep-ph].

[52] Miguel Escudero, Dan Hooper, Gordan Krnjaic, and Mathias Pierre, "Cosmology with A Very Light $L_\mu - L_\tau$ Gauge Boson," JHEP **03**, 071 (2019), arXiv:1901.02010 [hep-ph].

[53] P.S. Pasquini and O.L.G. Peres, "Bounds on Neutrino-Scalar Yukawa Coupling," Phys. Rev. D **93**, 053007 (2016), [Erratum: Phys.Rev.D 93, 079902 (2016)], arXiv:1511.01811 [hep-ph].

SUPPLEMENTAL MATERIAL

A. Matching Conditions

In this section, we provide the details on the matching conditions among the three time scales defined in the main text, z_A, z_B, z_C. This allows us to derive the time (z) dependence of the active neutrino temperature $T_\nu(z)$ and chemical potential $\mu_\nu(z)$.

At time z_A, the active neutrinos have just decoupled from the thermal plasma of other SM particles, thus $T_\nu(z_A) = T_\nu^{\rm sc}(z_A) \simeq 1\,{\rm MeV}$ and $\mu_\nu(z_A) = 0$. The corresponding energy and number densities of active neutrinos are

$$\rho_\nu(z_A) = \frac{7\pi^2}{80}T_\nu(z_A)^4, \quad n_\nu(z_A) = \frac{9\zeta(3)}{4\pi^2}T_\nu(z_A)^3 \ . \quad (13)$$

Here we count neutrinos and antineutrinos separately, i.e., $\rho_{\bar\nu} = \rho_\nu$, $n_{\bar\nu} = n_\nu$. Meanwhile, there also exist a sub-thermal population of ϕ that was frozen in via its interaction with active neutrinos. The corresponding values, denoted by $\rho_\phi(z_A)$ and $n_\phi(z_A)$, can be obtained by numerically solving Eq. (5).

The time z_B is defined when ϕ has just entered chemical equilibrium with active neutrinos. At this moment, the ϕ-ν system shares the same temperature $T_\nu(z_B)$, and also develops chemical potential where $\mu_\phi(z_B) = 2\mu_\nu(z_B)$. The corresponding energy, number, and entropy densities are
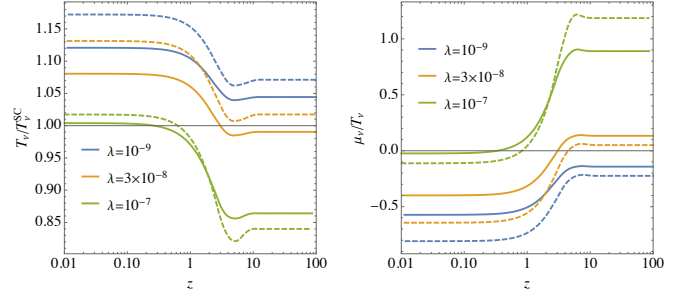

FIG. 3. Evolution of ratios $T_\nu(z)/T_\nu^{\rm sc}(z)$ and $\mu_\nu(z)/T_\nu(z)$ as functions of z for three values of λ_ϕ and holding $m_\phi = 5\,{\rm keV}$ fixed. Solid (dashed) curves correspond to real (complex) scalar ϕ case.

$$\rho_\nu(z_B) = -\frac{9T_\nu(z_B)^4}{\pi^2}{\rm Li}_4(-e^{\mu_\nu(z_B)/T_\mu(z_B)}) \ ,$$

$$n_\nu(z_B) = -\frac{3T_\nu(z_B)^3}{\pi^2}{\rm Li}_3(-e^{\mu_\nu(z_B)/T_\mu(z_B)}) \ ,$$

$$s_\nu(z_B) = -\frac{12T_\nu(z_B)^3}{\pi^2}{\rm Li}_4(-e^{\mu_\nu(z_B)/T_\mu(z_B)})$$
$$\qquad + \frac{3\mu_\nu(z_B)T_\nu(z_B)^2}{\pi^2}{\rm Li}_3(-e^{\mu_\nu(z_B)/T_\mu(z_B)}) \ ,$$

$$\rho_\phi(z_B) = \frac{3T_\nu(z_B)^4}{\pi^2}{\rm Li}_4(e^{2\mu_\nu(z_B)/T_\mu(z_B)}) \ ,$$

$$n_\phi(z_B) = \frac{T_\nu(z_B)^3}{\pi^2}{\rm Li}_3(e^{2\mu_\nu(z_B)/T_\mu(z_B)}) \ ,$$

$$s_\phi(z_B) = \frac{4T_\nu(z_B)^3}{\pi^2}{\rm Li}_4(e^{2\mu_\nu(z_B)/T_\mu(z_B)})$$
$$\qquad - \frac{2\mu_\nu(z_B)T_\nu(z_B)^2}{\pi^2}{\rm Li}_3(e^{2\mu_\nu(z_B)/T_\mu(z_B)}) \ ,$$
$$\qquad\qquad\qquad\qquad\qquad\qquad\qquad (14)$$

where we treat ϕ as an ultra-relativistic species ($m_\phi \ll T_\nu$), which is a good approximation throughout the parameter space we explore in this work. Again, in the case where ϕ is a complex scalar, the densities of the ϕ^* degree of freedom are counted separately. In the absence of CP violation, $\rho_{\phi^*} = \rho_\phi$, $n_{\phi^*} = n_\phi$, $s_{\phi^*} = s_\phi$.

The matching conditions between z_A and z_B are dictated by energy and lepton number conservation [29]. If ϕ is a real scalar, it comes to chemical equilibrium with both ν and $\bar\nu$, thus

$$\frac{\rho_\nu(z_A) + \rho_{\bar\nu}(z_A) + \rho_\phi(z_A)}{\rho_\nu(z_B) + \rho_{\bar\nu}(z_B) + \rho_\phi(z_B)} = \frac{z_B^4}{z_A^4} \ ,$$

$$\frac{n_\nu(z_A) + n_{\bar\nu}(z_A) + 2n_\phi(z_A)}{n_\nu(z_B) + n_{\bar\nu}(z_B) + 2n_\phi(z_B)} = \frac{z_B^3}{z_A^3} \ . \quad (15)$$

Alternatively, if ϕ is a complex scalar, it only comes into

equilibrium with neutrinos (ϕ^* equilibrates with $\bar{\nu}$), thus

$$\frac{\rho_\nu(z_A) + \rho_\phi(z_A)}{\rho_\nu(z_B) + \rho_\phi(z_B)} = \frac{z_B^4}{z_A^4} \; ,$$
$$\frac{n_\nu(z_A) + 2n_\phi(z_A)}{n_\nu(z_B) + 2n_\phi(z_B)} = \frac{z_B^3}{z_A^3} \; . \tag{16}$$

By definition $z_A/z_B = T_\nu^{\rm sc}(z_B)/T_\nu^{\rm sc}(z_A)$, and noting that $T_\nu(z_A) = T_\nu^{\rm sc}(z_A)$, the above set of equations (15) or (16) allows us to derive the ratios

$$\frac{T_\nu(z_B)}{T_\nu^{\rm sc}(z_B)}, \quad \frac{\mu_\nu(z_B)}{T_\nu(z_B)} \; . \tag{17}$$

In particular, in the case of real ϕ and with a negligible population of ϕ at time z_A (corresponds to a tiny λ), we can derive

$$T_\nu(z_B)/T_\nu^{\rm sc}(z_B) \simeq 1.12, \quad \mu_\nu(z_B)/T_\nu(z_B) \simeq -0.57 \; , \tag{18}$$

consistent with the findings of Ref. [30].

As the next step, we consider the evolution of T_ν and μ_ν between z_B and z_C, where z_C is defined as a temperature much lower than m_ϕ. During this epoch, the ν-ϕ system remains in chemical equilibrium. As a result, we can describe their thermal distributions at any time z where $z_B < z < z_C$. Because neutrino masses are still negligible, their energy, number and entropy densities are described by the same functions as those in Eq. (14), by simply replacing $z_B \to z$. On the other hand, the mass of ϕ becomes important and the corresponding distribution functions are evaluated using

$$\rho_\phi(z, m_\phi) = \frac{T_\nu(z)^4}{2\pi^2} \int_{\frac{m_\phi}{T_\nu(z)}}^{\infty} \frac{\left[x^2 - (m_\phi/T_\nu(z))^2\right]^{1/2} x^2 dx}{e^{x - \mu_\phi(z)/T_\nu(z)} - 1} \; ,$$

$$n_\phi(z, m_\phi) = \frac{T_\nu(z)^3}{2\pi^2} \int_{\frac{m_\phi}{T_\nu(z)}}^{\infty} \frac{\left[x^2 - (m_\phi/T_\nu(z))^2\right]^{1/2} x dx}{e^{x - \mu_\phi(z)/T_\nu(z)} - 1} \; ,$$

$$p_\phi(z, m_\phi) = \frac{T_\nu(z)^4}{2\pi^2} \int_{\frac{m_\phi}{T_\nu(z)}}^{\infty} \frac{\left[x^2 - (m_\phi/T_\nu(z))^2\right]^{3/2} dx}{e^{x - \mu_\phi(z)/T_\nu(z)} - 1} \; ,$$

$$s_\phi(z, m_\phi) = \frac{\rho_\phi(z, m_\phi) + p_\phi(z, m_\phi)}{T_\nu(z)} - \mu_\phi(z) n_\phi(z, m_\phi) \; , \tag{19}$$

where $\mu_\phi = 2\mu_\nu$ still holds.

Applying the matching conditions between z_B and z ($z_B < z < z_C$), which are entropy and lepton number conservation

$$\frac{s_\nu(z_B) + s_{\bar\nu}(z_B) + s_\phi(z_B)}{s_\nu(z) + s_{\bar\nu}(z) + s_\phi(z, m_\phi)} = \frac{z^3}{z_B^3} \; ,$$
$$\frac{n_\nu(z_B) + n_{\bar\nu}(z_B) + 2n_\phi(z_B)}{n_\nu(z) + n_{\bar\nu}(z) + 2n_\phi(z, m_\phi)} = \frac{z^3}{z_B^3} \; , \tag{20}$$

for the case of a real ϕ, or

$$\frac{s_\nu(z_B) + s_\phi(z_B)}{s_\nu(z) + s_\phi(z, m_\phi)} = \frac{z^3}{z_B^3} \; ,$$
$$\frac{n_\nu(z_B) + 2n_\phi(z_B)}{n_\nu(z) + 2n_\phi(z, m_\phi)} = \frac{z^3}{z_B^3} \; , \tag{21}$$

for the complex ϕ, and using the relation $z_B/z = T_\nu^{\rm sc}(z)/T_\nu^{\rm sc}(z_B)$, we will able to derive the ratio $\mu_\nu(z)/T_\nu(z)$, and $r(z)$ which is defined as

$$\frac{T_\nu(z)}{T_\nu^{\rm sc}(z)} = r(z) \frac{T_\nu(z_B)}{T_\nu^{\rm sc}(z_B)} \; . \tag{22}$$

Combining this result with the findings in Eq. (17), we can derive the ratio of neutrino temperatures in this model to that in standard cosmology, $T_\nu(z)/T_\nu^{\rm sc}(z)$.

For example, in the limit where $z = z_C \gg 1$ such that $\rho_\phi, n_\phi, s_\phi \to 0$ are all Boltzmann suppressed, for real scalar ϕ and negligible population of ϕ at z_A, we obtain

$$T_\nu(z_C)/T_\nu^{\rm sc}(z_C) \simeq 1.04, \quad \mu_\nu(z_C)/T_\nu(z_C) \simeq -0.14 \; , \tag{23}$$

also consistent with Ref. [30].

In Fig. 3, we show the evolution of T_ν and μ_ν as functions of z for three sets of model parameters. For very small λ, the asymptotic values are consistent with the results in Eq. (18) and (23). For sufficiently large λ, the freeze in population of ϕ (via Eq. (5)) before BBN is non-negligible which affects the matching results from z_A to z_C. The trend is also consistent with the limit where ϕ already thermalizes before BBN. In that case, we would have $z_A = z_B$ and $\mu_\nu(z_B) = 0$.

With the above results, we calculate the SνDM relic density using Eq. (7) in the main text. In Fig. 4, we plot the time dependence of $d\Omega_{\nu_4}/d\ln z$ for a few sets of model parameters. In all cases, we find that SνDM is dominantly produced around $z \simeq 3 - 4$ where ϕ already starts to become non-relativistic. If ϕ and ν_4 is nearly
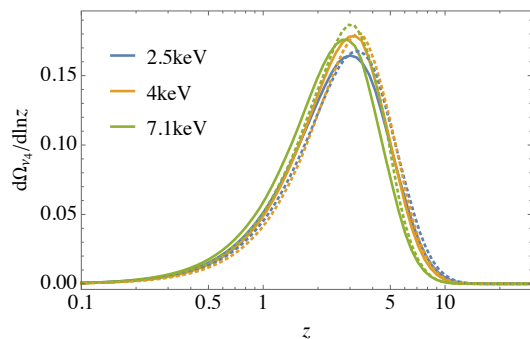

FIG. 4. Time dependence of SνDM, for three values of m_4 as labelled. The other parameters are chosen for producing the observed DM relic density. The solid (dashed) curves correspond to real (complex) scalar ϕ case.

degenerate ($m_\phi \gtrsim m_4$), SνDM will be produced with a velocity $v \ll c$.

Furthermore, the above results also allow us to calculate ΔN_{eff} at CMB time. After ϕ decays away at $z_C \gg 1$, the ratios $T_\nu(z_C)/T_\nu^{\mathrm{SC}}(z_C)$ and $\mu_\nu(z_C)/T_\nu(z_C)$ approach to constant values throughout the later evolution of the Universe, as shown in Fig. 3. We plug these functions into Eq. (11) of the main text. In the case of negligible ϕ population by the time of BBN, the value of $\Delta N_{\mathrm{eff}}^{\mathrm{CMB}}$ is 0.12 and 0.19 for real and complex ϕ case, respectively. The result for the real scalar case is consistent with the findings in Refs. [29].
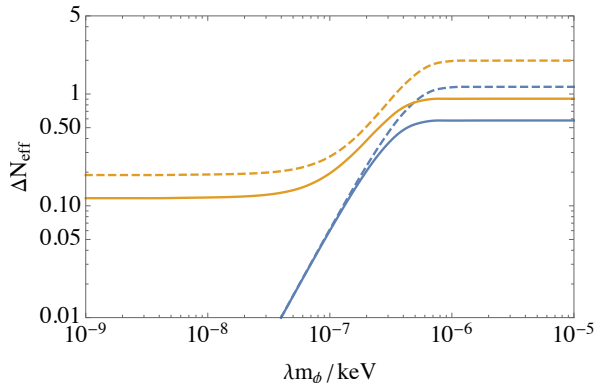

FIG. 5. Parametrical dependence of $\Delta N_{\mathrm{eff}}^{\mathrm{CMB}}$ (orange) and $\Delta N_{\mathrm{eff}}^{\mathrm{BBN}}$ (blue) on the product λm_ϕ, for real (solid) and complex (dashed) scalar cases. This result is valid as long as $m_\phi \ll 1\,\mathrm{MeV}$.

We observe that $\Delta N_{\mathrm{eff}}^{\mathrm{BBN}}$ and $\Delta N_{\mathrm{eff}}^{\mathrm{CMB}}$ depend on model parameter space λ and m_ϕ only through the combination λm_ϕ as long as the product is small (corresponding to the low-left half of Fig. 1). This dependence and the parametrical correlation are shown in Fig. 5 for real and complex scalars. We see that for sufficiently small λm_ϕ, there is no impact on $\Delta N_{\mathrm{eff}}^{\mathrm{BBN}}$ (blue curves) – no abundance of ϕ has developed by the time of BBN. On the contrary, even for $\lambda m_\phi \approx 10^{-9}\,\mathrm{keV}$, $\Delta N_{\mathrm{eff}}^{\mathrm{CMB}}$ has a lowest value, 0.12 or 0.19, depending on whether ϕ is real or complex due to distortions of the active neutrino distributions. For both BBN and CMB, large enough λm_ϕ results in a complete saturation of ΔN_{eff} and these curves level off to their maxima. This approximation is only valid for $m_\phi \ll 1\,\mathrm{MeV}$, where ϕ cannot decay away before BBN.

B. Minimal ΔN_{eff}

Here we provide some further context for the procedure used in generating Fig. 2 of the main text. For a given m_4, we determine the largest allowed $\sin^2(2\theta)$ assuming current limits from X-ray searches [2, 33–35], as well as the projected upper limit by Athena [37]. For a concrete choice, let us consider $m_4 = 2.5\,\mathrm{keV}$. The current limit

on this mass is $\sin^2(2\theta) < 5 \times 10^{-9}$, whereas Athena will have sensitivity at the level of $\sin^2(2\theta) = 10^{-10}$. We determine, for those two values of $\sin^2(2\theta)$, the preferred region of λ vs. m_ϕ parameter space for which ν_4 can account for all of the DM observed today – this is shown as the two solid black lines in Fig. 6. Each of those curves, near the minimum in λ realized, attains some minimum value of both $\Delta N_{\mathrm{eff}}^{\mathrm{CMB}}$ and $\Delta N_{\mathrm{eff}}^{\mathrm{BBN}}$. For the case we have considered here, $m_4 = 2.5\,\mathrm{keV}$, we find that with current limits on $\sin^2(2\theta)$, $\Delta N_{\mathrm{eff}}^{\mathrm{BBN}}$ ($\Delta N_{\mathrm{eff}}^{\mathrm{CMB}}$) must be at least 0.02 (0.14), and with future constraints (assuming Athena does not observe a signal compatible with $m_4 = 2.5\,\mathrm{keV}$) will require $\Delta N_{\mathrm{eff}}^{\mathrm{BBN}} > 0.4$ ($\Delta N_{\mathrm{eff}}^{\mathrm{CMB}} > 0.6$). In Fig. 6 we have assumed ϕ to be a real scalar, but the procedure is the same for complex ϕ. These minimum values are what is shown for that choice of m_4 in the left (current constraint on $\sin^2(2\theta)$) and right (post-Athena constraint) panels of Fig. 2.
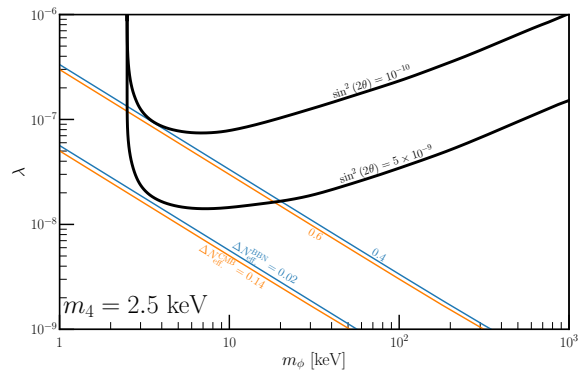

FIG. 6. Similar to Fig. 1 but with $m_4 = 2.5\,\mathrm{keV}$, $\sin\theta = 5 \times 10^{-9}$ and 10^{-10} for DM relic density calculation (black curves). The corresponding lowest values of $\Delta N_{\mathrm{eff}}^{\mathrm{CMB}}$ and $\Delta N_{\mathrm{eff}}^{\mathrm{BBN}}$ are shown by the orange and blue curves, respectively. Here we consider the real scalar ϕ case.

C. The Big Picture

To place the results of this work in a more complete picture, we present Fig. 7, with a wide range of m_ϕ between keV and 100 GeV. Like before, we assume that ϕ is a real scalar and couples equally to all neutrino flavors. For SνDM relic density, we choose $m_4 = 4\,\mathrm{keV}$ and $\sin^2(2\theta) = 10^{-9}$ (same as Fig. 1). On the black curve in Fig. 7, SνDM can make up all the dark matter in the Universe. The low mass ($m_\phi < 1\,\mathrm{MeV}$) part of the curve is determined by the approach described in this work, whereas the high mass part ($m_\phi > \mathrm{MeV}$) is obtained following Ref. [3]. There is a slight mismatch between the two parts of the curve around $m_\phi \sim \mathrm{MeV}$ (black dashed curve), due to the electron decoupling that makes an impact on the photon-neutrino temperature ratio.
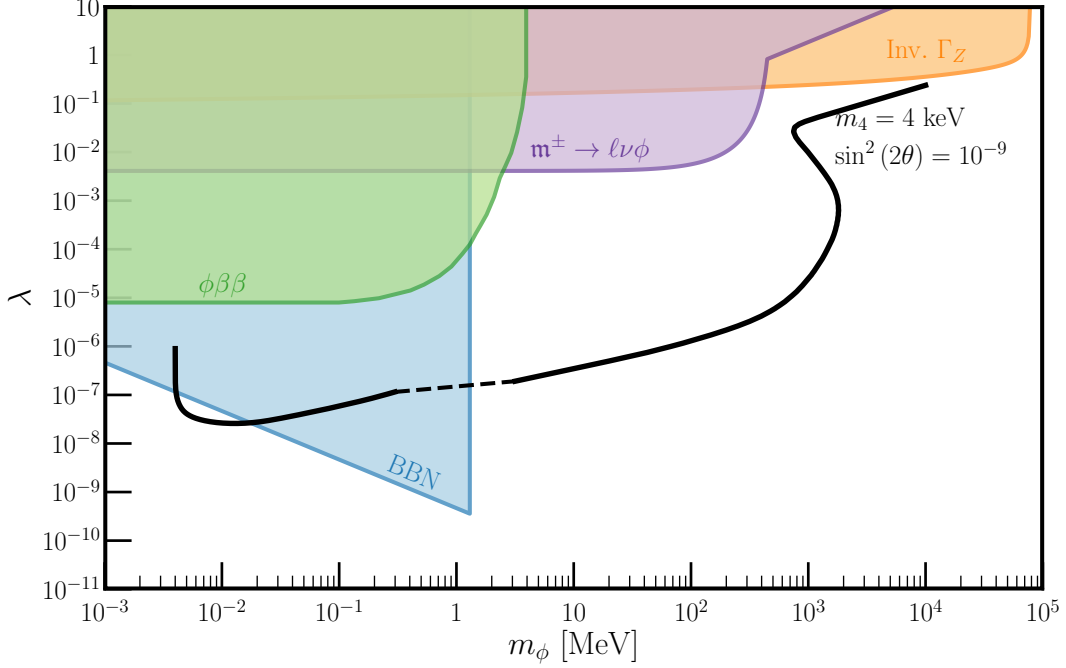
FIG. 7. The whole parameter space for sterile neutrino dark matter relic density (solid black curve) with $m_4 = 4$ keV and $\sin^2(2\theta) = 10^{-9}$, in the parameter space of mediator mass m_ϕ versus the $\phi - \nu$ coupling λ. Constraints from BBN (blue) and laboratory-based probes ($2\nu 2\beta$ decay in green, rare meson decays in purple ($\mathfrak{m} = K, \pi$), and the invisible width of the Z boson in orange) are shown for comparison. Here we assume ϕ to be a real scalar.

Regarding the mass range of ϕ, it cannot be heavier than 10-100 GeV because of the experimental upper bound (see discussion below) on the coupling λ. On the other hand, ϕ is also constrained to be not lighter than the SνDM (whose mass is constrained to be higher than ~ 2 keV) to avoid the BBN bound (blue shaded region). The black curve sweeps across the λ-m_ϕ plane if we vary m_4 and $\sin^2 2\theta$.

Constraints from laboratory-based probes are shown for comparison, including emission of ϕ that contributes to the $2\nu 2\beta$ rate (green) [42–44], rare decays of charged mesons with ϕ emission (purple) [5, 15, 53], and contributions to the invisible width of the Z boson [17]. The shaded blue region, labelled "BBN", corresponds to $\Delta N_{\text{eff}}^{\text{BBN}} = 0.5$, a conservative upper limit on this value at BBN epochs [36].